

Synthesis and optical properties of the glassy compound $As_{0.63}S_{2.70}Sb_{1.37}Te_{0.30}$

M. Iovu^a, I. Culeac^a, V. Verlan^a, Olga Bordian^a, M. Enachescu^{b,d},
A. A. Popescu^{c,*}, D. Savastru^c, A. Lazar^d

^a*Institute of Applied Physics, Str. Academiei 5, MD-2028 Chisinau, R. Moldova*

^b*Center for Surface Science and Nanotechnology, University Politehnică of Bucharest, Splaiul Independentei 313, Bucharest, 060042 Romania*

^c*National Institute of Research and Development for Optoelectronics INOE 2000, Str. Atomistilor 409, 077125, Magurele, Romania*

^d*S.C. NanoPRO START MC S.R.L., 110310 Pitesti, Romania*

The amorphous chalcogenide semiconductor $As_{0.63}S_{2.70}Sb_{1.37}Te_{0.30}$ was synthesized and thin films based on it were obtained. XRD and optical images investigations showed the amorphous and homogeneous nature of the samples. The optical transmission spectrum in the UV-Vis range of $As_{0.63}S_{2.70}Sb_{1.37}Te_{0.30}$ thin films shows good transparency in the spectral range 0.7-3.5 μm with a single absorption threshold at 2.05 eV and with refractive index in infrared 2.3. The irradiation of films with light leads to a parallel shift of the transmission spectrum to the IR range. The materials with $As_{0.63}S_{2.70}Sb_{1.37}Te_{0.30}$ composition have high optical transparency that make they promises for applications in holographic memory devices, optical amplitude and phase recorder, optical processing units and others.

Received March 15, 2023; Accepted May 31, 2023)

Keywords: Chalcogenide glasses, $As_{0.63}S_{2.70}Sb_{1.37}Te_{0.30}$, UV-VIS transmission

1. Introduction

Multicomponent glasses based on *As-S-Sb-Te* are intensively studied due to the ability to form new optical properties such as increased structural stability, flexibility, elasticity, etc. [1]. They are beginning to be widely applied in optoelectronics as infrared optical elements, as materials for image creation and holographic information storage, acousto-optical elements, optical memory switches [2,3], X-ray imaging [4] etc. These materials are less affected by temperature because they have a low level of phonons and have heavy anions. Sulphur, selenium and tellurium are the main components of their compositions. Multicomponent glasses are also being studied for applications in passive and active devices such as fiber laser amplifiers and nonlinear components [1]. Chalcogenide materials exhibit unique properties such as photodarkening, huge photoexpansion, and photofluidity when irradiated by appropriate light. Also, glasses are prone to non-linear optical properties.

This paper presents the extension of our previous experimental studies [5,6] regarding new chalcogenide materials in quaternary As-S-Sb-Te system. As shown in our early paper [5] chalcogenide materials, which have the composition similar to this one, namely $As_{11.2}S_{48.0}Sb_{28.8}Te_{12.0}$ and $As_{20.8}S_{48.0}Sb_{19.2}Te_{12.0}$ demonstrate polycrystalline structure. Thereby, the task of obtaining complex chalcogenide materials with high homogeneity remains a topical issue. In order to combine the advantages of short distance and medium-intermediate distance and with the increase of flexibility and elasticity in a single composition, in this paper an optimal quaternary vitreous compound with composition $As_{0.63}S_{2.70}Sb_{1.37}Te_{0.30}$ was obtained. Optical properties of thin films obtained by thermal vacuum evaporation were studied.

* Corresponding author: apopescu@inoe.ro
<https://doi.org/10.15251/CL.2023.205.387>

2. Experimental part and discussion

2.1. Synthesis of glassy material

All chemicals were purchased from Aldrich Chemical Co. The glassy chalcogenide semiconductor $As_{0.63}S_{2.70}Sb_{1.37}Te_{0.30}$ was synthesized using the elements *As*, *S*, *Sb*, *Te* with a purity of (99.999%), in quartz ampoules. The precursors were weighed, loaded into the ampoule which was then evacuated, vacuum sealed (10^{-5} mm Hg) and placed in the oven. The furnace temperature was slowly raised at a rate of $1^{\circ}\text{C}/\text{min}$ up to 920°C . The maximum temperature of the liquid melt mixture was maintained for 12 hours along with the rotation of the furnace around the perpendicular axis to obtain a homogeneous mass. Subsequently, melt quenching was applied. The ampoule was suddenly cooled by removing it from the oven to room temperature. Parts of the synthesized ingot were ground into powder with grain sizes of about 100 nm for microscopic measurements and thin films preparation. The measurements of the elemental thin film's composition in different places of the sample showed the same composition, which further confirms the elemental homogeneity of the sample.

Table 1. EDX statistics of the elemental composition of the composite $As_{0.63}S_{2.70}Sb_{1.37}Te_{0.30}$.

Elements:	<i>S</i>	<i>As</i>	<i>Sb</i>	<i>Te</i>
Calculated, %	13.93	25.55	49.23	11.29
Average measured, %	12.73	25.05	50.06	11.72

2.2. Preparation of thin films

The thin films were thermally deposited by vacuum evaporation (10^{-5} mm Hg) using a "quasi-closed" complex molybdenum evaporator. A special cover with many holes is provided in the construction of the vaporizer to ensure a uniform flow on the substrate so that a uniform film thickness can be obtained over an area of 100 cm^2 [7, 8]. For this purpose, the VUP-4 vacuum plant was equipped with the recording and maintenance of the evaporator temperature.

Temperature control was carried out automatically with the VRT-2 temperature regulator. The films were obtained on optical glass substrates. The evaporation temperature of the $As_{0.63}S_{2.70}Sb_{1.37}Te_{0.30}$ material was constant during the evaporation which ensured the maintenance of a constant condensation rate during the evaporation period. The thickness of the deposited layers was determined by the evaporation time. The thickness homogeneity was regulated by diaphragms mounted above the evaporator. The uniform thickness distribution over the whole layer was also ensured by selection of distance between the substrate and the evaporator. The distance between the evaporator and the substrate was equal to 21 cm. Transparent amorphous films with thicknesses of $125 \div 1000$ nm were obtained. The films thickness was measured using the MII-4 interferometric microscope. The structure of bulk material and thin films investigated by the XRD method shows the absence of any sharp line diffraction, indicating that the nature of the material is amorphous. The elemental analysis studied by EDX [9] and shown in Table 1 confirmed the composition of the material $As_{0.63}S_{2.70}Sb_{1.37}Te_{0.30}$. Phillips [10], Mott [11] and Flank et al. [12] showed that the coordination number of atoms with covalent bonds in glass is determined by the 8-N rule, where N is the number of electrons in the outer electronic shell [21]. The 8-N rule suggests that the number of nearest neighbor atoms for (*S*, *Te*) and (*As*, *Sb*) are two and three respectively. As calculation shows, the nearest neighbor atoms number for chosen $As_{0.63}S_{2.70}Sb_{1.37}Te_{0.30}$ composition of material is similar to As_2S_3 number of neighbor atoms.

2.3. Optical transmission

UV-VIS transmission measurements were performed at room temperature on samples of $As_{0.63}S_{2.70}Sb_{1.37}Te_{0.30}$ thin films, using a Perkin Elmer UV/VIS/IR-960 spectrometer.

The system uses a grid PMT with a Peltier-controlled PbS detector to perform high-performance tests in the spectral range up to 3300 nm. UV-VIS resolution reaches 0.05 nm, while NIR resolution reaches up to 0.2 nm. Absorption/transmission spectra for all samples were recorded in the 400–3300 nm range.

The optical transmission spectrum $T(\lambda)$ of the thin layer of $As_{0.63}S_{2.70}Sb_{1.37}Te_{0.30}$ ($T(\lambda)$) in the range 500 – 3500 nm is shown in Fig. 1.

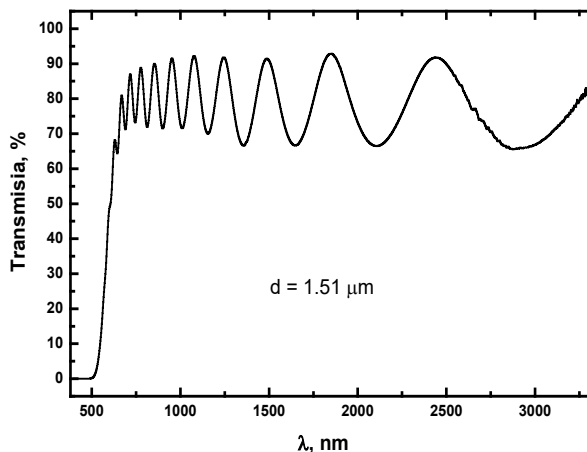


Fig. 1. The transmission spectrum of the $As_{0.63}S_{2.70}Sb_{1.37}Te_{0.30}$ layer.

It is formed by a steep threshold in the range 500 – 550 nm followed by the range of 550–3500 nm where $T(\lambda)$ is oscillatory. From the spectrum of transmission in the transparency region the absorption coefficient α , the refractive index n and the layer thickness d were calculated using the method of Swanepoel [13]. The interference effects occur due to multiple reflections between the interfaces of a thin film with air and substrate, when the thickness of the film is close to the coherence length of the light. This effect produces an interference pattern in the transmission spectrum. At wavelengths longer than the bandgap and neglecting the absorption and scattering of light in the IR range, the maximum transmission values correspond to the transmittance of the substrate alone, while the minimum transmission occurs when the reflections from the two surfaces of the film interfere in the opposite phase.

The refractive index of the chalcogenide layer (n) (Fig. 2) was calculated from the transmission data according to the formula [9]:

$$n = [N + (N^2 - n_s^2)^{1/2}]^{1/2} \quad (1)$$

$$N = 2n_s (T_M - T_m) / T_M T_m + (n_s^2 + 1)^{1/2} \quad (2)$$

where T_M and T_m are the maximum and minimum transmission values, and n_s is the refractive index of the substrate (for glass $n_s = 1.5$).

Film thickness was determined by examining the distance between adjacent maxima and minima using the following equation: $d = k\lambda_k$ where d is the film thickness, $\lambda_k = (\lambda_M + \lambda_m)/2$ is the wavelength and k is the order number. Maxima occurs at integer values of the order number, and minima occur at half integers [9].

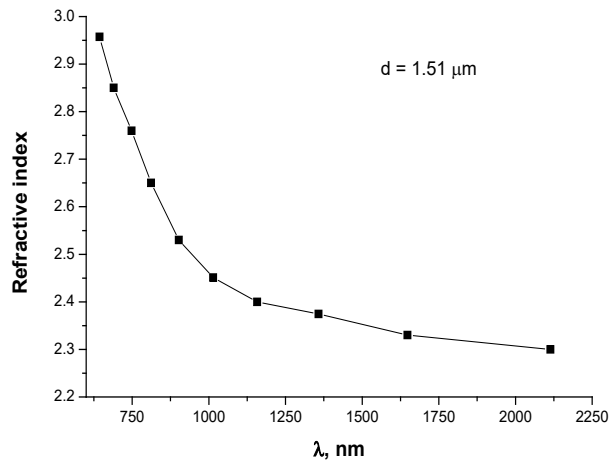


Fig. 2. Refractive index versus wavelength for $As_{0.63}S_{2.70}Sb_{1.37}Te_{0.30}$ amorphous compound.

2.4. Optical absorption

The absorption coefficient (Fig. 3) was determined according to the formula $\alpha = -\ln(T(\lambda))/d$, where $T(\lambda)$ is the transmission coefficient, and d is the layer thickness. The optical absorption spectrum is the important tool for studying the band gap of the material. The optical absorption edge (the value of the forbidden band E_g) was analysed by the following relation [14]:

$$(\alpha h\nu) = A(h\nu - E_g)^m \quad (3)$$

where A is the fringe width parameter characterizing the film quality.

Optical energy gap of the material is calculated from the tangent of the linear part of this relationship. Calculations made from the graph give for A the value of $700 \text{ eV}^{-1/2} \text{ cm}^{-1/2}$. The index m is determined by type of optical transition in material. As is well known, the parameter m has the value $1/2$ for direct transition allowed and two for indirect transition allowed.

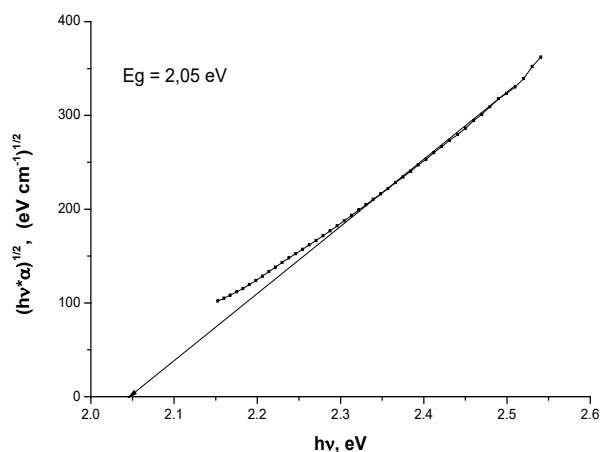


Fig. 3. Processed absorption spectrum for films of the composition $As_{0.63}S_{2.70}Sb_{1.37}Te_{0.30}$.

The method of determination the type of transition involves a graphical representation of the relations $(\alpha h\nu)^2$ or $(\alpha h\nu)^{1/2}$ versus $h\nu$ [15, 16]. The straight line was obtained for the dependence $(\alpha h\nu)^{1/2} = f(h\nu)$ as shown in Fig. 3, which means that indirect transitions are allowed.

The bandgap (optical activation edge) E_g was determined by intersection of extrapolate linear dependence of the graph $(\alpha h\nu)^{1/2} = A(h\nu - E_g)$ with the $h\nu$ axis. The bandgap of 2.05 ± 0.1 eV for this compound was determined from the graph.

2.5. The sensitivity to the irradiation with violet light

The glassy film of composition $As_{0.63}S_{2.70}Sb_{1.37}Te_{0.30}$ was exposed to the violet light illumination of the 30 W lamp for 15 min. After that the transmission spectrum was measured. As is shown in Fig. 4 photoinduced parallel shift of the $T(\lambda)$ spectrum towards the infrared range by about 50 nm is observed. These induced effects can be used to form various optical components including waveguides and surface gratings, homo- and heteronuclear bonds that produce the amorphous density of state defects. The doubly covalently bonded chalcogen atom possesses a lone pair of electrons, which does not bond completely in the glass. These bonds are broken under UV illumination and the its number are change after relaxation.

The glassy film of composition $As_{0.63}S_{2.70}Sb_{1.37}Te_{0.30}$ was exposed to the violet light illumination of the 30 W lamp for 15 min. After that the transmission spectrum was measured. As is shown in Fig. 4 photoinduced parallel shift of the $T(\lambda)$ spectrum towards the infrared range by about 50 nm is observed. These induced effects can be used to form various optical components including waveguides and surface gratings, homo- and heteronuclear bonds that produce the amorphous density of state defects.

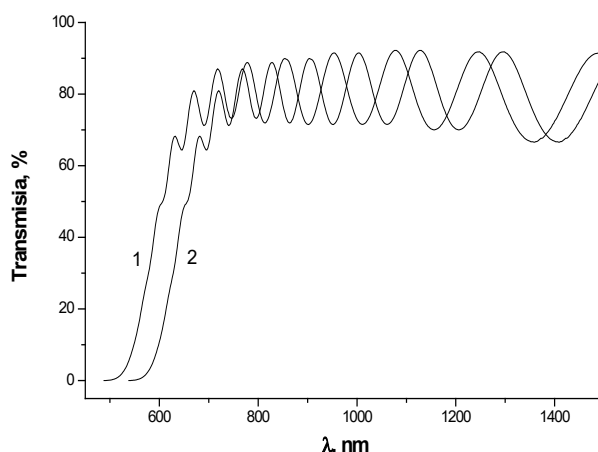


Fig. 4. Transmission sensitivity (1) without irradiation and (2) upon irradiation with violet light ($\lambda = 405$ nm) for 15 min.

The doubly covalently bonded chalcogen atom possesses a lone pair of electrons, which does not bond completely in the glass. These bonds are broken under UV illumination and the its number are change after relaxation.

3. Conclusions

The amorphous glassy semiconductor $As_{0.63}S_{2.70}Sb_{1.37}Te_{0.30}$ was synthesized and thin films layers were obtained. The composition of thin films practically reproduces composition of bulk. The amorphous material possesses both high homogeneity and high optical transparency. Photoinduced changes in transmission spectrum under UV illumination were investigated. The dispersion of the refractive index was obtained for a wide spectral range. From the absorption spectrum interpreted as indirect transitions the 2.05 eV value of optical bandgap was obtained. The thin films obtained from the synthesized material possessed large photoinduced changes of transmission under UV irradiation. Due to that, the $As_{0.63}S_{2.70}Sb_{1.37}Te_{0.30}$ amorphous compound can be proposed for application in memory devices and registration media.

Acknowledgments

This work was funded by ANCD Moldova through projects 20.80009.5007.14, 22 80013.5007.6BI, by European Union through projects ECSEL: H2020 MADEin4 (Ctr. no. 8/1.1.3H/06.01.2020, code POC-SMIS 128826), ECSEL -H2020 OCEAN12 (Ctr. no. 9/1.1.3H/20.01.2020, POC-SMIS code 129948), ECSEL-H2020 PIN3S (Ctr. no. 10/1.1.3H/03.04.2020, POC-SMIS code 135127). This work was carried out through the Core Program within the National Research Development and Innovation Plan 2022-2027, carried out with the support of MCID, project no. PN 23 05, Exploratory Research grant number PN-III-P4-PCE-2021-0585 and by the Romanian Ministry of European Investment and Projects & Romanian Ministry of Research, Innovation and Digitalization, contract no.8/1.2.1 PTI ap.2/17.02.2023.

References

- [1] Savage J. A., *J Non-Cryst Solids*, vol. 47 (1), 101 (1982); [https://doi.org/10.1016/0022-3093\(82\)90349-0](https://doi.org/10.1016/0022-3093(82)90349-0)
- [2] A. Christy Ferdinand, M.S. Shekhawat, In book Kurt Binder and Walter Kob, *Glassy Materials and Disordered Solids: An Introduction to Their Statistical Mechanics*, World Scientific, Hackensack, NJ, 171 (2005).
- [3] B. G. Sangeetha, A.G. Gayathri et al., *Materials Today-Proceedings*, 2999 (2017); <https://doi.org/10.1016/j.matpr.2017.02.182>
- [4] A. Chirita, D. Spoiala, S.Vatavu, *Chalcogenide Lett.*, Vol. 19 (10),683 (2022); <https://doi.org/10.15251/CL.2022.1910.683>
- [5] J. S. Sanghera, Ishwar D. Aggarwal, L. B. Shaw et al., *J. Optoelectron. Adv. M.* vol. 8 (6) 2148 (2006).
- [6] Iaseniuc O., Iovu M., *Chalcogenide Lett.* vol. 19 (2), 117 (2022).
- [7] Iaseniuc O.V., Iovu M.S., *Proceedings of ICNBME-2021*, November 3-5, Chisinau, Moldova, 77 (2021); https://doi.org/10.1007/978-3-030-92328-0_11
- [8] A.A. Popescu A.A., D. Savastru, L. Bașchir, V.V. Verlan, O. Bordian, M. Stafe, N. Puscas, *Chalcogenide Lett*, vol. 17, 117 (2020).
- [9] Mihai Iovu, Victor Verlan, Olga Bordian, Marius Enachescu, Aurelian Popescu, Dan Savastru, Laura-Bianca Enache, Sabrina Rosoiu, Matei Bardeanu, Oana Andreea Lazar, Geanina Mihai, *Optoelectron. Adv. Mat.* **16**(11-12), 538 (2022).
- [10] J. C. Phillips, *J. Non-Cryst. Solids*, vol. 34, 153 (1979); [https://doi.org/10.1016/0022-3093\(79\)90033-4](https://doi.org/10.1016/0022-3093(79)90033-4)
- [11] N. F. Mott, *Philos Mag*, vol. 19, 835 (1969); <https://doi.org/10.1080/14786436908216338>
- [12] A. M. Flank, D. Bazin, H. Dexpert, P. Lagarde, C. Mervo & J. Y. Barraud, *J. Non-Cryst. Solids*, vol. 91, 306 1987; [https://doi.org/10.1016/S0022-3093\(87\)80341-1](https://doi.org/10.1016/S0022-3093(87)80341-1)
- [13] R. Swanepoel, *J. PHYS. E: Sci. Instrument*, vol. 16, 1214 (1983); <https://doi.org/10.1088/0022-3735/16/12/023>
- [14] J. Tauc, *The Optical Properties of Solids*, North-Holland Publishing, 171 (1972).
- [15] A. M. Andriesh, *Properties of chalcogenide glasses for optical waveguides*, *J Non-Cryst Solids*, vol. 77-78, part. 2, 1219 (1985); [https://doi.org/10.1016/0022-3093\(85\)90878-6](https://doi.org/10.1016/0022-3093(85)90878-6)
- [16] A. Andriesh, *J. Optoelectron. Adv. M.* **7**(6), 2931 (2005).